



**HAL**  
open science

# Pd-Catalyzed Coupling of Bromo-N-( $\beta$ -glucopyranosyl)quinolin-2-ones with Amides: Synthesis of N-glucosyl-6BrCaQ Conjugates with Potent Anticancer Activity

Wafa Redjdal, Sara Benmahdjoub, Thi Thanh Hyen Luong, Belkacem Benmerad, Franck Le Bideau, Juliette Vergnaud, Samir Messaoudi

## ► To cite this version:

Wafa Redjdal, Sara Benmahdjoub, Thi Thanh Hyen Luong, Belkacem Benmerad, Franck Le Bideau, et al.. Pd-Catalyzed Coupling of Bromo-N-( $\beta$ -glucopyranosyl)quinolin-2-ones with Amides: Synthesis of N-glucosyl-6BrCaQ Conjugates with Potent Anticancer Activity. *ChemMedChem*, 2024, 19 (15), pp.e202400195. 10.1002/cmde.202400195 . hal-04905231

**HAL Id: hal-04905231**

**<https://hal.science/hal-04905231v1>**

Submitted on 22 Jan 2025

**HAL** is a multi-disciplinary open access archive for the deposit and dissemination of scientific research documents, whether they are published or not. The documents may come from teaching and research institutions in France or abroad, or from public or private research centers.

L'archive ouverte pluridisciplinaire **HAL**, est destinée au dépôt et à la diffusion de documents scientifiques de niveau recherche, publiés ou non, émanant des établissements d'enseignement et de recherche français ou étrangers, des laboratoires publics ou privés.

# Pd-Catalyzed Coupling of Bromo-*N*-( $\beta$ -glucopyranpsyl)quinolin-2-ones with Amides: Synthesis of *N*-glucosyl-6BrCaQ Conjugates with Potent Anticancer Activity

Wafa Redjda,<sup>[a]</sup> Sara Benmahdjoub,<sup>[a], [b]</sup> Thi Thanh Hyen Luong,<sup>[c]</sup> Belkacem Benmerad,<sup>[a]</sup> Franck Le Bideau,<sup>[c]</sup> Juliette Vergnaud,<sup>[d]</sup> and Samir Messaoudi<sup>\*,[c][e]</sup>

[a] W. Redjda, Dr. S. Benmahdjoub, Dr. B. Benmerad  
Université de Bejaia, Faculté des Sciences Exactes,  
Laboratoire de Physico-Chimie des Matériaux et Catalyse,  
06000 Bejaia, Algeria

[b] Dr. S. Benmahdjoub  
Département de Chimie, Université M'Hamed Bougara de Boumerdes,  
35000 Boumerdes, Algeria

[c] Drs. T. T. H. Luong, F. Le Bideau, Dr. S. Messaoudi  
Université Paris-Saclay, CNRS, BioCIS, 92290, Orsay, France

[d] Dr. J. Vergnaud  
Université Paris-Saclay, CNRS, Institut Galien-Paris Saclay, 92290, Orsay, France

[e] Dr. S. Messaoudi  
Laboratoire de Synthèse Organique, Ecole Polytechnique, CNRS, ENSTA, Institut Polytechnique de Paris  
Palaiseau, France

E-mail: [samir.messaoudi@cnrs.fr](mailto:samir.messaoudi@cnrs.fr)

Supporting information for this article is given via a link at the end of the document. ((Please delete this text if not appropriate.))

**Abstract:** A series of *N*-glycosyl- 6BrCaQ conjugates was synthesized through a Pd-catalyzed cross-coupling reaction between brominated *N*-glycosyl quinolin-2-one derivatives and various nitrogen nucleophiles. Antiproliferative assays revealed that this new series of analogues represents a promising class of antitumor compounds as illustrated by the high biological activity observed for several derivatives towards different cancer cell lines compared to the non-glycosylated congeners.

## Introduction

Heat shock protein 90 (HSP90) has emerged as an attractive target for cancer therapy due to its critical role in maintaining the stability and function of numerous client proteins involved in cell survival and proliferation.<sup>1</sup> HSP90 is known to regulate the stability and function of several client proteins that play key roles in oncogenesis and tumor progression, including kinases, transcription factors, and proteins involved in cell cycle regulation and apoptosis. Thus, targeting HSP90 leads to disrupt multiple oncogenic pathways simultaneously, making it a promising therapeutic strategy.<sup>2</sup> HSP90 inhibitors bind to the *N*-terminal ATP-binding site of HSP90 (*N*-terminal domain, NTD), thereby preventing its conformational changes and inhibiting its chaperone function. This leads to the degradation of client proteins, including those that promote cell survival and drive tumor growth. Consequently, HSP90 inhibition can interfere with critical signaling pathways, induce cell cycle arrest, inhibit angiogenesis, and promote cancer cell death. Furthermore, the

ability of HSP90 inhibitors to target multiple client proteins can potentially overcome drug resistance, a major challenge in cancer treatment. The NTD Hsp90 inhibitors have shown promising results in preclinical and clinical studies, both as single agents and in combination with other cancer therapies. However, none of them is FDA-approved mainly because of an adverse response called Heat-Shock Response (HSR).<sup>3</sup> HSR is characterized by the release of the transcription factor Heat Shock Factor-1 (HSF-1) from HSP90 chaperoning after the inhibitor binding and the subsequent induction of the transcription of the genes coding HSP90, HSP70, and HSP27 leading to an increased protein expression.

Therefore, several groups focused their drug discovery research on inhibiting the *C*-terminal domain since it does not induce the release of HSF-1.<sup>4</sup> Novobiocin (Figure 1) was reported to bind weakly to the Hsp90 *C*-terminal ATP binding site (~700 M in SkBr3 cells) and to induce degradation of Hsp90 client proteins.<sup>5</sup> Structure-activity relationship studies allowed several groups to identify promising inhibitors with a mechanism of action distinct from *N*-terminal inhibitors. In this context, our group identified 6-BrCaQ (Figure 1) as a very promising *C*-terminal HSP90 inhibitor. This compound was active on various cancer cell lines with a IC<sub>50</sub> of 5-50  $\mu$ M,<sup>6</sup> inducing apoptosis and decreasing the levels of client proteins of HSP90 on prostate cancer cells, PC3. Besides, encapsulated in liposomes, 6BrCaQ exerted an improved *in vitro* activity on breast cancer cells (MDA-MB-231) and had an anti-tumor effect on an orthotopic breast cancer model in nude mice.<sup>7</sup> Moreover, we demonstrated recently that the conjugation of 6BrCaQ with the triphenyl phosphonium (TPP) function through

an alkyl C<sub>10</sub>-linker generates the 6BrCaQ-C10-TPP conjugate (Figure 1) for a selective TRAP1 machinery.<sup>8</sup> 6BrCaQ-C10-TPP displays the anti-proliferative activity with mean GI<sub>50</sub> values at a nanomolar level in a diverse set of human cancer cells (GI<sub>50</sub> = 0.008-0.30 μM) including MDA-MB-231, HT-29, HCT116, K562 and PC-3 cancer cell lines. In addition, 6BrCaQ-C<sub>10</sub>-TPP is able to interfere with TRAP1 function and to inhibit proliferation of colon carcinoma cells without inducing the heat-shock response HSF1.<sup>8</sup>

One of the most promising strategy in drug optimization approaches is the introduction of a sugar moiety in bioactive molecules which induces several advantages such as improving their bioavailability,<sup>9</sup> their solubility, or their biological activity by selectively targeting cancerous tissues through the overexpression of glucose transporters (GluT) on the surface of cancer cells.<sup>10</sup> Such approach has led to the approval of more than 170 carbohydrate-based drugs worldwide up to date including glufosfamide, paclitaxel, adriamycin, chlorambucil,...etc (Figure 1A).<sup>11</sup> Particularly, the HSP90 inhibitor Geldanamycin

(GA) was subjected to glycoconjugation and various carbohydrate-GA conjugates were synthesized.<sup>12</sup> While glucose-GA conjugate (Figure 1) showed anticancer activity through cleavage of glucose moiety by β-glucosidase inside of the cancer cells, galactose-GA conjugates remained inactive in the absence of exogenous β-galactosidase. However, their anticancer activity increased by 3- to 40-fold when incubated with β-galactosidase.

Inspired by this carbohydrate-drug conjugates strategy for cancer-specific targeting, we embarked in our group on a synthetic program to produce glucose-6BrCaQ conjugates of type 4 (Figure 1B). Our hypothesis is that the linkage of the sugar nucleus to the lead compound 6-BrCaQ might be able to increase the affinity of the drug inside the binding pocket leading thereby to a higher antiproliferative activity. Moreover, the presence of the sugar moiety may improve the solubility, the selectivity toward cancer cell lines as well as the pharmacokinetic properties.

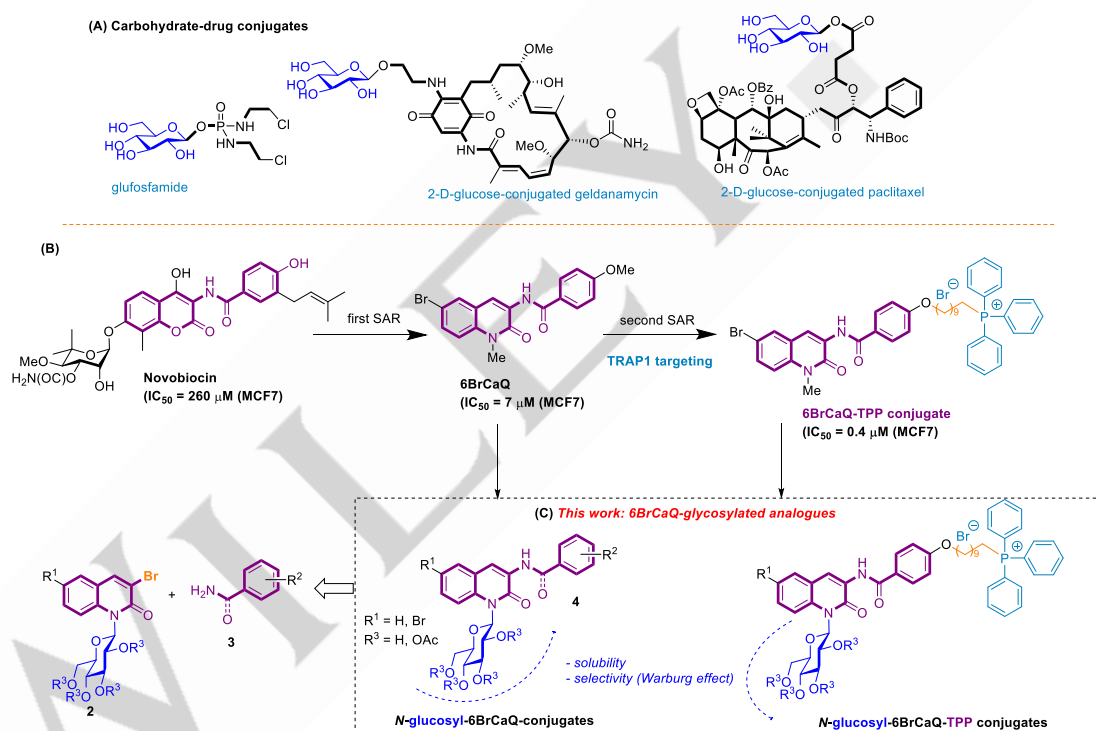


**Figure 1.** (A) Selected example of carbohydrate-drug conjugates, (B) structure of novobiocin, 6-BrCaQ and 6-BrCaQ-TPP, (C): our strategy against 6-BrCaQ-glucose conjugates.

Herein, we succeeded in modifying the previously synthesized HSP90 C-terminal inhibitor 6-BrCaQ by introducing a glucose moiety at the nitrogen atom of the quinolone scaffold. During this study, a synthetic methodology based on a Pd-catalyzed coupling of 3-bromo-N-glucosylated quinolinones **2** with various nitrogen nucleophiles **3** including aromatic and aliphatic amides as well as amines was developed. A series of glycoconjugate 6-BrCaQ analogues **4** were prepared and a preliminary *in vitro* efficacy of these compounds in terms of antiproliferative effect is reported. This study revealed that the introduction of the sugar nucleus

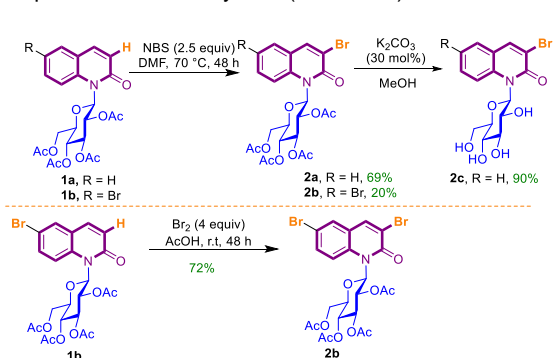
showed promising properties by increasing 10-fold the antiproliferative activity in various cancer cell lines.

## Result and discussion

### Synthesis of 3-bromo-N-glucosyl quinolin-2-ones **3a-c**

To establish appropriate conditions for the selective coupling of bromo-N-glucosylated quinolinones<sup>13</sup> **2a-c** with various nitrogen nucleophiles, **2a** and **3a** were initially selected as model

substrates (Table 1) to determine the optimized reaction conditions. To this end, the selective bromination of the *N*-glycosylquinolin-2-ones **1a**<sup>13</sup> was first performed at the 3-position through the electrophilic aromatic bromination by employing a freshly recrystallized *N*-bromosuccinimide (NBS) to produce the desired product **2a** in 69% yields (Scheme 1).



**Scheme 1:** Synthesis of (di)bromo-*N*-( $\beta$ -glucopyranosyl)quinolin-2-one **2a-c**.

Our study next focused on the synthesis of 3,6-dibromo-*N*-( $\beta$ -tetra-*O*-acetylglucopyranosyl)quinolin-2-one **2b** (Scheme 1). With compound **1b**<sup>13</sup> bearing a bromine atom at the 6-position in hand, the previously reported bromination conditions with NBS were inefficient, only 20% yield of the dibrominated product **2b** being obtained (Scheme 1). This result demonstrated that the presence of an electro-withdrawing substituent at the C6-position influences the outcome of the reaction. The examination of different reaction conditions revealed that when the reaction was carried out with Br<sub>2</sub> (4 equiv) in glacial acetic acid at room temperature, the 3,6-dibrominated-*N*-glucosylquinolinone **2b** was isolated selectively as a single product in excellent 72% yield (Scheme 1). Finally, the deprotected *N*-glucosyl quinolinone **2c** was prepared through a deprotection of the acetyl groups under basic conditions (Scheme 1).

### Synthesis of 3-amido-*N*-glycosyl quinolin-2-ones **4**

Next, we continued our study by exploring the feasibility of the key step C(sp<sup>2</sup>)-N bond formation by examining the different reaction conditions. The presence of the sugar moiety makes the coupling more challenging because of the possible chelation/interaction of this polyhydroxylated part to the catalyst, particularly with unprotected sugar, which might lead to a complete deactivation of the turnover of the catalyst.

We started this task by examining the coupling of **2a** with **3a** as a model study (Table 1). In a previous methodology, we reported a robust and efficient Pd-catalyzed amination/amidation method of bromoquinolinone to access a wide range of *N*-functionalized quinolinones.<sup>14</sup> However, applying these reported conditions (Pd(OAc)<sub>2</sub> (10 mol %), 20 mol% XantPhos at 100 °C in dioxane) to the coupling of **2a** with **3a** for a prolonged reaction time (24 h) did not afford the formation of the desired product **4a** (Table 1, entry 1). We were nevertheless pleased to find that increasing the temperature to 130 °C (entry 2) allowed the formation of **4a** in an excellent 91% yield within 15 minutes. Interestingly, the use of

only 5 mol% of the Pd-catalyst and 10 mol% of the XantPhos ligand furnished the desired product in a similar yield (88% yield, entry 3), while running the reaction for a longer time (30 min instead 15 min) led to a slight decrease of the yield (79 %, entry 4) probably due to the degradation of the formed product **4a**.

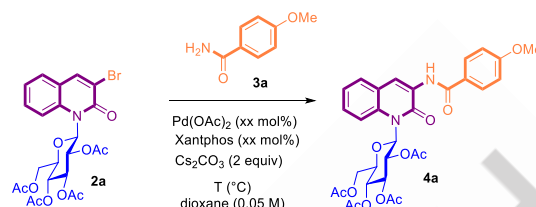


**Table 1.** Optimization of the coupling reaction of **2a** with 4-methoxybenzamide **3a**<sup>[a]</sup>

entry	Pd(OAc) <sub>2</sub>	XantPhos	Time (h)	T (°C)	Yield <sup>[b]</sup>
1	10 mol%	20 mol%	24	100	0
2	10 mol%	20 mol%	0.25	130	91
3	5 mol%	10 mol%	0.25	130	88
4	5 mol%	10 mol%	0.5	130	79
5	-	10 mol%	0.25	130	0
6	5 mol%	0	0.25	130	0

[a] Reactions were conducted with substrate **2a** (0.4 mmol), **3a** (1.2 mmol), Pd(OAc)<sub>2</sub> (n mol%), XantPhos (n mol%), Cs<sub>2</sub>CO<sub>3</sub> (2 equiv.) in a dioxane [0.05 M]. [b] Yield of isolated product **4a**.

Control experiments revealed that the use of a Pd-catalyst and ligand were necessary to achieve this transformation since no reaction took place when the coupling was conducted in their absence (entries 5 and 6).

Motivated by these results, we next explored the scope of this *N*-heteroarylation procedure. Owing to the cost of the Pd-metal and ligand, we privileged to use the conditions of entry 3 (5 mol% of Pd-catalyst and 10 mol% of the ligand) for the couplings of diverse amides with **2a** (Scheme 2).

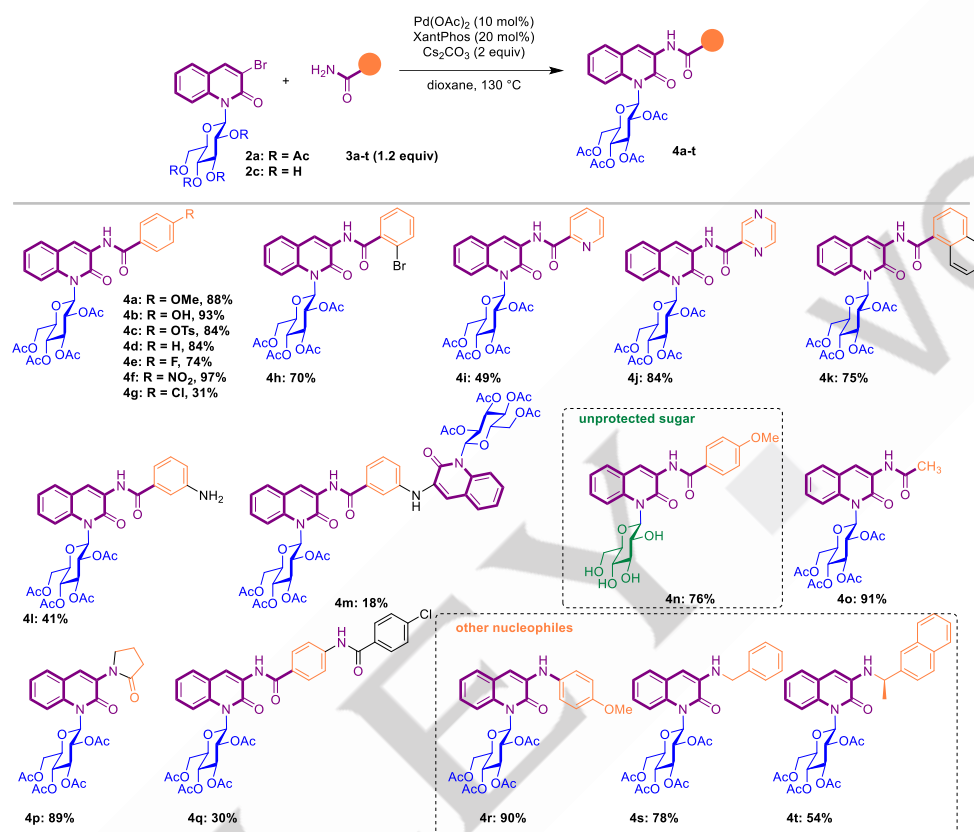
At first, we were pleased to see that various benzamides bearing diverse functions at the para-position such as -OMe, -OH, -OTs, -Cl, -Br, -F, -NO<sub>2</sub>, -NH<sub>2</sub>, reacted smoothly with **2a** to afford the desired 3-amido-*N*-glycosyl quinolin-2-ones **4a-h**, **4k** and **4l** in moderate to good yields while maintaining the  $\beta$ -anomeric stereoselectivity intact. Surprisingly, the presence of a bromo substituent at the *ortho* position of the aromatic ring of the coupling partner did not affect the reaction process, as the compound **4h** was obtained in 70% yield.

Interestingly, **2a** was subjected to the coupling with benzamide **3l** bearing an amino group at the *meta* position. Under our reaction conditions, the amide function proved to be more reactive than the aniline nucleophile leading to the 3-amido-*N*-glycosyl quinolin-2-one **4l** as a major product isolated in 40% yield. In addition, the di-coupling product **4q** was isolated in 18% yield. Again, the formation of the di-coupling product **4m** was (Scheme 2) also

observed in 30% yield when 4-chlorobenzamide **3g** was used as a coupling partner.

Moreover, heterocyclic benzamides such as pyridine **3i** and pyrazine **3j** were also tolerated producing **4i** and **4j** in 49% and 84% yield, respectively. Besides, alkyl amides such as methylamide **3o** and pyrrolidinone **3p** are also effective partner delivering the corresponding products **4o** and **4p** in excellent yields (91% and 89%, respectively).

Importantly, performing the coupling reaction between 3-bromoquinolinone **2c** bearing an unprotected sugar unit, with the benzamide **3a** produces the desired product **4n** in 76% yield. The latter can be regarded as a non-brominated *N*-glucose-6BrCaQ conjugate. Finally, different other nucleophiles including anisidine **3r**, and benzylamines **3s** and **3t** were used with success during this methodology delivering the 3-amino-*N*-glycosyl quinolin-2-ones **4r-t** in yields ranging from 54% to 90% (Scheme 2).



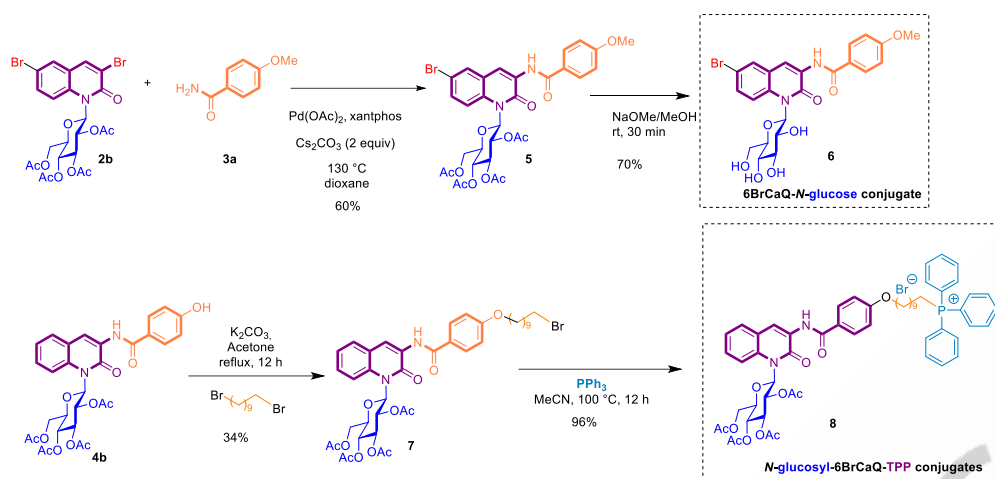
**Scheme 2.** Palladium-catalyzed amidation/amination of *N*-glycosylated 3-bromoquinolin-2-ones **2a,c**.

Encouraged by the efficiency of our C(sp<sup>2</sup>)-N bond forming methodology, we decided to apply it to the synthesis of both protected and unprotected *N*-glucose-6BrCaQ conjugates **5** and **6** (Scheme 3). The *O*-acetylated analogue **5** can be considered as a pro-drug of **6** because the ester functions of the sugar unit can be cleaved by esterase enzymes in the biological medium to deliver the free-hydroxylated drug **6**.

Thus, analogue 6-bromo-3-benzamido-*N*-(β-tetra-*O*-acetylglucopyranosyl)quinolin-2-one **5** was prepared in good 60% yield starting from tetra-*O*-acetylated quinolinone **2b** and *p*-methoxy-benzamide **3a** under our optimized cross-coupling conditions. The Zampfen deprotection of acetate groups of compound **5** furnished the direct 6BrCaQ-glucose conjugate **6** in 70% yield.<sup>15</sup>

Another important application of this method is the preparation of the *N*-glycosylated derivative **8** (Scheme 3) as an analogue of 6BrCaQ-C10-TPP conjugate in order to explore the selective targeting of TRAP1 protein. To this end, reaction of the phenol **4b** (Figure 2) with a large excess of 1,10 dibromodecane (8–10 equiv.) in the presence of potassium carbonate at acetone reflux furnished selectively the mono-alkylated compound **7** in a synthetically useful yield (Scheme 3). The second C-Br bond was functionalized by a nucleophilic substitution in the presence of triphenylphosphine to produce the desired glycosylated 6BrCaQ-C10-TPP **8** in 96% yield.





**Scheme 3.** Synthesis of compounds 6 and 8 as molecules of potential biological interest

### Biological study

Upon completion of syntheses, the *in vitro* activity of compounds 4a-t, 5, 6 and 8 was evaluated by their growth-inhibitory potency against human colon carcinoma HCT-116 cells at concentrations of 10<sup>-5</sup> M (10 μM) and 10<sup>-6</sup> M (1 μM) in comparison with 6BrCaQ. The quantification of cell survival in this cell line was established by using CellTiter Glo® (Promega) which allows the measurement of the number of living cells by luminescence (transformation of luciferin to oxyluciferin in the presence of ATP). This method determines the number of viable cells in culture based on quantitation of the ATP (an indicator of metabolically active cells). The amount of ATP is directly proportional to the number of cells present in the culture.

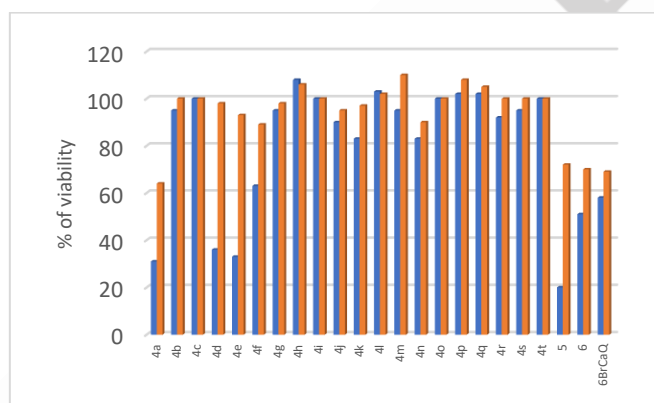


**Figure 2.** *In vitro* viability of HCT116 cells towards compounds 4a-q, 5 and 6 at two concentrations (10 μM, blue columns and 1 μM, orange columns). Qualification of cell survival was established after 72 h exposure. These results were expressed in percentage of viable cells compared to untreated cells 100%. Data are the mean ± SE (n = 3).

The results are expressed in Figure 2 as viability percentage. A lower percentage of viability means that the compound is more active. Five molecules (4a, 4d, e, 5, 6) significantly display an anti-proliferative effect when compared to 6BrCaQ (survival less than 50%) in the growth of HCT-116 cells at 10 μM concentration. At this stage, these preliminary results revealed that in the glycosylated series of 6BrCaQ, the presence of the bromine atom at the C6-position of the quinolinone is not necessary to induce a

similar anti-proliferative activity while in the non-glycosylated series, removing the bromine atom led to the total loss of the biological activity.

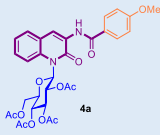
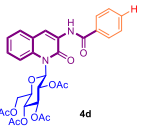
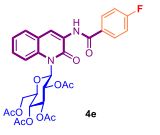
Another interesting observation is that from the benzamide side, the presence of a fluorine atom at the *para* position induces a similar effect to the methoxy group (31% and 32% survival at 10 μM, respectively), however, replacing the -OMe by a hydroxyl group (4b) leads to a total loss of the activity (90% survival at 10 μM). The other substituents at the *para* position of the benzamides such as -OTs, -Cl, -NO<sub>2</sub> were not active. In addition, the heterocyclic benzamides 4i,j as well as other nitrogen functions (lactam 4p, acetamide 4o, anisidine 4r and benzylamines 4s,t) revealed to be not active too (> 90% survival at 10 μM).

Surprisingly, derivative 4n bearing an unprotected sugar unit did not show any anti-proliferative activity (>90% survival at 10 μM) while both protected *N*-glucosyl congeners 4a and 5 lead to a higher reduction in cell viability than 6BrCaQ at 10 μM concentration with 31%, 20% and 62% of viability respectively. Moreover, the deprotected conjugate 6 is less efficient being close to our lead compound 6BrCaQ both at 1 and 10 μM (70% vs 69% at 1 μM and 51% vs 58% at 10 μM).

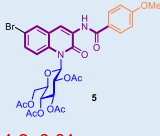
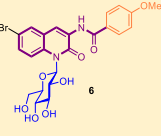
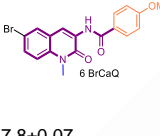
With these very promising results in hands, we next investigated the dose-response relationship between the concentration of these compounds and cell viability in order to evaluate their IC<sub>50</sub> against colon cancer (HCT116), prostate cancer (PC-3) and human chronic myelogenous leukemia (K562) cell lines (Table 2). Compound 4a and its brominated derivative 5 exhibit excellent anti-proliferative activity against human colon carcinoma (HCT116) and human immortalized myelogenous leukemia (K562) cell lines with IC<sub>50</sub> values between 0.89 and 12.4 μM. Notably, HCT116 cell lines showed the most sensitive viability to protected analogues (IC<sub>50</sub> = 0.89 μM for molecule 4a, 1.28 μM for molecule 5 and 5.55 μM for molecule 4e). These results demonstrate that the presence of a bromine atom at the C6 position is not required since compound 4a exhibits similar activity to its brominated congener 5. They also revealed that colon cancer HCT116 and leukemia K562 cells are more sensitive to acetylated compounds 4a and 5 than the unprotected one 6. This could be explained by the high polarity of the sugar unit which induces a less cell membrane crossing than the acetylated

prodrug congeners. Surprisingly, the three *N*-glycosylated molecules **4a**, **5** and **6** did not show any anti-proliferative activity against PC-3 cell lines (> 100  $\mu\text{M}$ ) compared to **6BrCaQ** ( $\text{IC}_{50}$  = 44  $\mu\text{M}$ ) indicating that the presence of a sugar moiety suppresses the anti-proliferative activity against this cancer cell line. The carbohydrate metabolism in prostate cancer cells may be a possible explanation for such a result.<sup>16</sup>

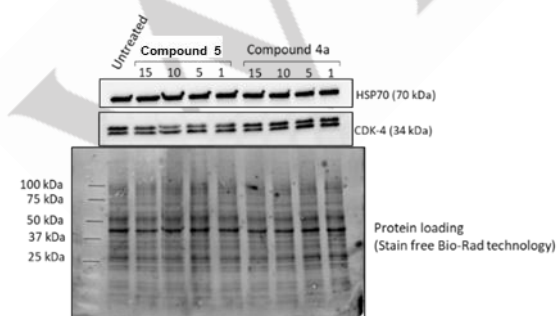
**Table 2.** Values of  $\text{IC}_{50}$  ( $\mu\text{M}$ ) of compounds **4a**, **4d**, **4e**, **5** and **6** against HCT-116, K562 and PC-3 cancer cell lines measured by the CellTiter Glo (Promega).

			
HCT116	0.9±0.005	59.8±5.15	5.5±0.11
K562	12.4±0.41	nd	nd
PC-3	>100	nd	nd

			
HCT116	1.3±0.01	79.1±0.24	7.8±0.07
K562	2.6±0.34	22.7±0.66	47.7±3.39
PC-3	>100	>100	44±5.81

To investigate the impact of **4a** and **5** on the chaperon machinery, we performed a western blots experiment to establish the expression profile of the Hsp70 chaperon which functions upstream of Hsp90 in the chaperon machinery. As shown in Figure 3, Hsp70 is not induced after the treatment with **4a** and **5** in HT29 ( $\text{IC}_{50}$  estimated to 5  $\mu\text{M}$  by MTT assay). The level of Hsp70 was similar to that obtained in control conditions (untreated cells) for concentrations up to 15  $\mu\text{M}$  of **4a** and **5**. In addition, compound **4a** induces a slightly down-regulation of CDK-4 from only 5  $\mu\text{M}$ , while **5** doesn't affect the CDK4 expression. These results suggest that both compounds **4a** and **5** may exhibit their

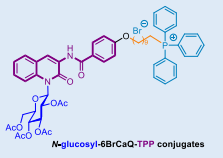
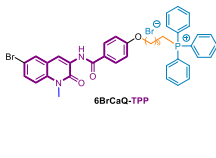


**Figure 3:** Effect of compounds **4a** and **5** on Hsp70 and CDK-4 protein expression. Cells were seeded for 24 h then incubated for 24 h with liposomal **6BrCaQ** (1, 5, 10 and 15  $\mu\text{M}$ ). untreated cells were used as control. Hsp70 and CDK4 protein expressions were analyzed by signal intensity measurements.

biological activity through a different mode of action than was previously described for compounds **6BrCaQ** by affecting the downregulation of other HSP90 client proteins such as Her2 or Raf-1 or by interaction with various clusters of Hsp90 client proteins as suggested for celastrol, which preferentially affects the Hsp90–cdc37 interaction.<sup>17</sup>

TRAP1 is a very important therapeutic target, and treatment with TRAP1 inhibitors combined with chemotherapeutic agents may become a new therapeutic strategy for cancer. In this context, gamitrinib derivatives which combines the HSP90 inhibitor Geldanamycin with TPP as a mitochondrial targeting moiety, was shown to selectively induce apoptosis of prostate cancer cells, including chemo-resistant ones, without damaging normal cells.<sup>18</sup> Our group reported recently the use of the same approach to target the mitochondrial HSP90 TRAP1. The combination of **6BrCaQ** with the triphenyl phosphonium (TPP) function through an alkyl  $\text{C}_{10}$ -linker generates the **6BrCaQ-C10-TPP** conjugate (Figure 1) with very high anti-proliferative activity at the nanomolar level against various human cancer cells ( $\text{GI}_{50}$  = 0.008–0.30  $\mu\text{M}$ ).<sup>8</sup> Encouraged by this study, we synthesized the derivative **13** as a glucosylated analogue of **6BrCaQ-C10-TPP** and examined its activity against 5 cancer cell lines in comparison with the original molecule **6BrCaQ-C10-TPP** (table 3). Pleasingly, derivative **8** showed a higher activity than **6BrCaQ-C10-TPP** demonstrating that the sugar unit plays an important role in the biological activity. Interestingly, these two molecules showed different behaviors depending the cancer cells. While both compounds displayed a similar anti-proliferative activity against cancer cell lines MDA-MB-231 and leukemia cells K562 (Table 3), the cytotoxicity of **8** toward PC-3 and MCF-7 (85 nM and 55 nM, respectively) is 4 to 7-fold higher than **6BrCaQ-C10-TPP** (350 nM and 390 nM respectively). In contrary, **6BrCaQ-C10-TPP** is more active on HCT-116 than **8** (65 nM vs 680 nM).

**Table 3.** Values of  $\text{IC}_{50}$  ( $\mu\text{M}$ ) of **6BrCaQ-C10-TPP** and their sugar analogue **8** against MDA-MB-231, MCF7, HCT-116, K562 and PC-3 cancer cell lines measured by the CellTiter Glo (Promega).

entry		
MDA-MB-231	0.064±0.004	0.045±0.005
K562	0.03±0.004	0.035±0.0002
PC-3	0.085±0.005	0.35±0.006
MCF7	0.055±0.07	0.40±0.02
HCT116	0.70±0.01	0.065±0.006

## Conclusion

In conclusion, we have developed an efficient  $\text{C}(\text{sp}^2)\text{-N}$  Buchwald-Hartwig bond forming reaction to access to *N*-glycosyl-6BrCaQ derivatives. This procedure exhibits broad substrate scope with respect to the nucleophilic partners. This methodology,

we also applied to the synthesis of glucosylated analogue of **6BrCaQ-C10-TPP** in order to selectively target the mitochondria TRAP1 protein. Among these molecules, we identified several derivatives with good to excellent anti-proliferative activities against MDA-MB-231, MCF7, HCT-116, K562 and PC-3 cell lines below the  $\mu\text{M}$  level.

## Supporting Information

The authors have cited additional references within the Supporting Information.<sup>[19, 20]</sup>

## Acknowledgements

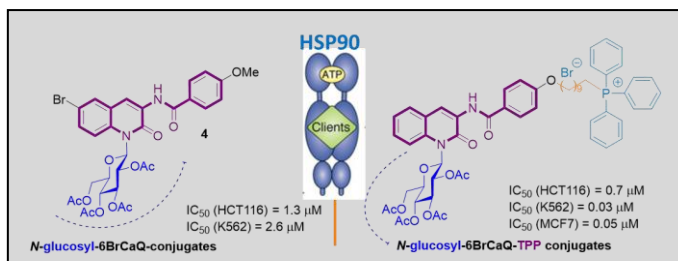
Authors acknowledge support of this project by CNRS and University Paris-Saclay. We also thank the Algerian Ministry of Education and Research for a fellowship (PNE) to Sara Benmahdjoub and Wafa Redjald.

**Keywords:** *N*-glycosides • HPS90 • TRAP1 • Buchwald-Hartwig Cross-Coupling • Antiproliferative activity

- [1] F. H. Schopf, M. M. Biebl, J. Buchner, *Nat. Rev. Mol. Cell Biol.* **2017**, *18*, 345; b) G. Chiosis, C. S. Digwal, J. B. Trepel, L. Neckers, *Nat. Rev. Mol. Cell Biol.* **2023**, *24*, 797;
- [2] Z.-N. Li, Y. Luo, *Oncol Rep.* **2023**; *49*, 6.
- [3] Y. C. Koay, J. R. McConnell, Y. Wang, S. J. Kim, L. K. Buckton, F. Mansour, S. R. McAlpine, *ACS Med. Chem. Lett.* **2014**, *5*, 771.
- [4] a) R. L. Matts, A.; Dixit, Peterson, L. Sun, S. Voruganti, P. Kalyanaraman, S. D.; Hartson, G. M.; Verkhivker, B. S. J. Blagg, *ACS Chem. Biol.* **2011**, *6*, 800; b) Z.; Zhang, Z. You, R. T. Dobrowsky, B. S. J. Blagg, *Bioorg. Med. Chem. Lett.* **2018**, *28*, 2701; c) S. Terracciano, A. Russo, M. G.; Chini, M. C. Vaccaro, M. Potenza, A. Vassallo, R. Riccio, G. Bifulco, I. Bruno, *Sci. Rep.* **2018**, *8*, 1709; d) S. Y.; Hyun, H. T.; Le, C.-T.; Nguyen, Y.-S.; Yong, H.-J.; Boo, H. J.; Lee, J.-S.; Lee, H.-Y.; Min, J.; Ann, J.; Chen, H.-J.; Park, J.; Lee, H.-Y. Lee, *Sci. Rep.* **2018**, *8*, 13924; Y. Wang, S. R. McAlpine, *Chem. Commun.* **2015**, *51*, 1410.
- [5] M. G. Marcu, A. Chadli, I. Bouhouche, M. Catelli, L. M. Neckers, *J. Biol. Chem.* **2000**, *275*, 37181.
- [6] a) D.; Audisio, S. Messaoudi, L. Cegielski, J.-F. Peyrat, J.-D.; Brion, D. Methy-Gonnot, C. Radanyi, J.-M. Renoir, M. Alami, *ChemMedChem* **2011**, *6*, 804; b) D. Audisio, D. Methy-Gonnot, C. Radanyi, J.-M.; Renoir, S. Denis, F. Sauvage, J. Vergnaud-Gauduchon, J.-D. Brion, S. Messaoudi, M. Alami, *Eur. J. Med. Chem.* **2014**, *83*, 498.
- [7] F. Sauvage, S. Franzè, A. Bruneau, M. Alami, S. Denis, V. Nicolas, S. Lesieur, F.-X. Legrand, G. Barratt, S. Messaoudi, J. Vergnaud-Gauduchon, *Int. J. Pharm.* **2016**, *499*, 101; c) F. Sauvage, E.; Fattal, W. Al-Shaer, S. Denis, E.; Brotin, C. Denoyelle, Blanc- C. Fournier, B. Toussaint, S. Messaoudi, M. Alami, G. Barratt, J. Vergnaud-Gauduchon, *Cancer Lett.* **2018**, *432*, 103.
- [8] C. Mathieu, Q. Chamayou, T. T. H. Luong, D. Naud, F. Mahuteau-Betzer, M. Alami, E. Fattal, S. Messaoudi, J. Vergnaud-Gauduchon, *Eur. J. Med. Chem.* **2022**, *229*, 114052
- [9] S. V. Moradi, W. M. Hussein, P. Varamini, P. Simerska, I. Toth, *Chem. Sci.* **2016**, *7*, 2492
- [10] a) E. C. Calvaresi, P. J. Hergenrother, *Chem. Sci.* **2013**, *4*, 2319; b) F. Hossain, P. R. Andreada, *Pharmaceuticals* **2019**, *12*, 84; c) J. Fu, J. Yang, P. H. Seeberger, J. Yin, *Carbohydr. Res.* **2020**, *498*, 108195.
- [11] a) X. Cao, X. Du, H. Jiao, Q. An, R. Chen, P. Fang, J. Wang, B. Yu, *Acta Pharm. Sin. B* **2022**, *12*, 3783 b) L. Pan, C. Cai, C. Liu, D. Liu, G. Li, L. R. J. inhardt, G. Yu, *Curr. Opin. Biotechnol.* **2021**, *69*, 191
- [12] H.; Cheng, X. Cao, M. Xian, Fang, T.B. Cai, J.J. Ji, J.B. Tunac, D. Sun, P.G. Wang, *J. Med. Chem.* **2005**, *48*, 645
- [13] T. T. H. Luong, J.-B. Brion, E. Lescop, M. Alami, S. Messaoudi, *Org. Lett.* **2016**, *18*, 2126
- [14] S. Messaoudi, D. Audisio, J.-D. Brion, A. Alami, *Tetrahedron*, **2007**, *63*, 10202.
- [15] G. Zemplén, A. Kunz, *Chem. Ber.* **1924**, *57B*, 1357
- [16] P. L. Martin, J. J. Yin, V. Seng, O. Casey, E. Corey, C. Morrissey, R. M. Simpson, K. Kelly, *Oncogene* **2017**, *36*, 525
- [17] a) T. Zhang, A. Hamza, X Cao, B. Wang, S. Yu, C. G. Zhan, D. Sun, *Mol. Cancer Ther.* **2008**, *7*, 162 b) A. Chadli, S. J. Felts, Q. Wang, W. P. Sullivan, M. V. Botuyan, A. Fauq, M. Ramirez-Alvarado, G. Mer, *J. Biol. Chem.* **2009**, *285*, 4224 c) K. Eckert, J.-M. Saliou, L. Monlezun, A. Vigouroux, N. Atmane, C. Caillat, S. Quevillon-ChØrueel, K. Madiona, M. Nicaise, S. Lazereg, A. Van Dorsselaer, S. Sanglier-CianfØrani, P. Meyer, S. MorØra, *J. Biol. Chem.* **2010**, *285*, 31304.
- [18] a) F. C. Fiesel, E. D. James, R. Hudec, W. Springer *Oncotarget.* **2017**, *8*, 106233; b) U. Hayat, G. T Elliott, A. J Olszanski, D. C Altieri, *Cancer Biol Ther.* **2022**, *23*, 117.



## Entry for the Table of Contents



A series of *N*-glycosyl-quinolinone-carboxamides conjugates for HSP90 targeting were designed. Their synthesis was achieved through a simple and efficient Buchwald-Hartwig cross coupling and their antiproliferative activities revealed that this new series of analogues represents a promising class of antitumor compounds.

Institute and/or researcher Twitter usernames: @samuccen